Long-Distance Structural Consequences of H-Bonding. How H-Bonding Affects Aromaticity of the Ring in Variously Substituted Aniline/Anilinium/Anilide Complexes with Bases and Acids†

Halina Szatyłowicz,*,‡ Tadeusz M. Krygowski,§ and Joanna E. Zachara-Horeglad§

Faculty of Chemistry, Warsaw University of Technology, Noakowskiego 3, 00-664 Warsaw, Poland, and Department of Chemistry, Warsaw University, Pasteura 1, 02-093 Warsaw, Poland

Received November 9, 2006

The aromaticity of the ring in variously substituted aniline/anilinium/anilide derivatives in their H-bonded complexes with various Broensted acids and bases was a subject of an analysis based on 332 experimental geometries retrieved from the Cambridge Structural Database and geometries optimized at the B3LYP/6-311+G** and MP2/aug-cc-pVDZ levels of theory. Ab initio modeling was applied to the para-substituted aniline, anilinium cation, and anilide anion derivatives (X = NO, NO_2, CN, CHO, H, CH_3, OCH_3, and OH) and their H-bonded complexes (only for X = NO, NO_2, CHO, H, and OH) with B (B = F^- and CN^-) or HB (HB = HF and HCN). In both cases, the harmonic oscillator model of aromaticity index (HOMA) was used, whereas for computational geometries, additionally, the magnetism-based indices NICS, NICS(1), and $NICS(1)_{zz}$ were also applied (NICS = nucleus-independent chemical shift). There is an equivalent prediction of aromaticity by NICSs and HOMA and approximate monotonic dependences of HOMA and NICS on the C−N bond length. The strongest changes in aromaticity estimated by HOMA and NICSs were found for aniline derivatives with $NH_2\cdots$B and anilide derivatives without and with $NH^-\cdots$HB interactions. The changes observed for two other kinds of interactions, $NH_2\cdots$HB and $NH_3^+\cdots$base (for anilinium cations), are much smaller. For all four kinds of interactions, the relationships between ipso-bond angle, mean ipso-ortho bond length, and C−N bond length follow the Bent−Walsh rule.

INTRODUCTION

In spite of some ambiguity and disputation concerning the definition of aromaticity, it is a widely used term related to the stability and π-electron delocalization of a great variety of π-electron systems.[1−5] For a recent review, see Bultinck.[6] Aromatic properties as well as geometry patterns of the benzene ring in its various derivatives have been the subject of many investigations.[7] It was found that changes in geometry of the ring due to the substituent effect concentrate mainly at the ipso and both ortho bond angles[8,9] and depend on the electronegativity of the substituent.[10] Aromaticity of the ring depends weakly on substituent effects,[11] with the exception of the cases where the empty $2p_z$ orbital or the $2p_z$ electron pair in the substituent interacts strongly with the π-electron system of the ring.[12] The effect is enhanced for para-disubstituted benzene derivatives in which the substituents are of opposite properties: electron-accepting and electron-donating.[13]

It has been shown recently that aromaticity of the ring in phenol derivatives in H-bonded complexes with various bases changes dramatically.[14−16] It was shown that the more acidic the phenol derivative is, the greater is the decrease of aromaticity of the ring estimated by means of the geometry-based harmonic oscillator model of aromaticity index (HOMA)[3,17] and magnetism-based nucleus-independent chemical shift index (NICS).[18−20]

Aniline differs from phenol in that it can act stronger as the Broensted base (in water, for conjugated acid $C_6H_5NH_3^+$, pK_a = 4.596 and 9.99 for phenol)[21] and also weaker as an acid (pK_a = 30.6 and 18.0 for aniline and phenol, respectively, in DMSO).[22] The $NH_2\cdots$base interactions were used by Kamlet and Taft[23] to define the β-scale of solvent basicity. The more basic the solvent is, the greater is the red-shift of the long band in the UV/vis spectra: the lone pair on the nitrogen atom needs less energy for n → π^* electron excitation. Acidic properties of the N−H bond in aniline are shown by its Reichardt's normalized solvent polarity parameter,[24] E_T^N, which is equal to 0.42, whereas for phenol, this parameter is 0.70. In this scale, water has E_T^N = 1.00, and tetramethyl silane has E_T^N 0.00. Reichardt's polarity parameter may be considered as a measure of Lewis acidity properties of solvents.[23,25] The nitrogen atom with its lone pair is an excellent proton acceptor forming H-bonds.[26] Additionally, in acidic media, aniline can form the anilinium cation in which N−H may also be involved in H-bonding as a proton donor (see Chart 1), and in strongly basic media, aniline can form the anilide anion in which, negatively charged, the nitrogen atom acts as a strongly basic center.

H-bonding is ubiquitous and one of the most important kinds of interactions.[4d,27] Most studies are associated with its properties, criteria of existence, and consequences, particularly in biosphere and life and material sciences.[28]

† Dedicated to Professor Nenad Trinajstić on the occasion of his 70th birthday.

* Corresponding author phone: (+48) 22 234 77 55; fax: (+48) 22 628 27 41; e-mail: halina@ch.pw.edu.pl.

‡ Warsaw University of Technology.

§ Warsaw University.

10.1021/ci600502w CCC: $37.00
Published on Web 04/20/2007

Chart 1[a]

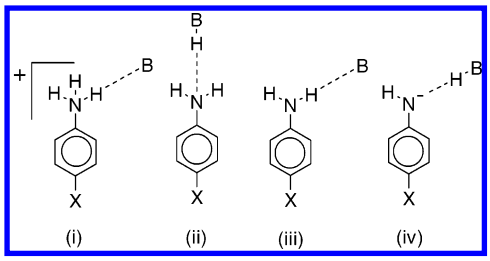

[a] X = NO, NO_2, CHO, H, OH; B = F^-, CN^-; HB = HF, HCN

Fewer papers deal with long-distance structural consequences observed in H-bond-accepting or H-bond-donating systems as a whole.[14,15,29,30]

The purpose of this work is to analyze how the above-mentioned four kinds of H-bonding affect the aromaticity of the ring in aniline, anilinium cation, and anilide anion derivatives involved in H-bonded complexes. As a basis for our study, we have used experimental geometries retrieved from the Cambridge Structural Database (CSD)[31] and geometries obtained from computational modeling[32] for the complexes presented in Chart 1.

METHODOLOGY

Geometries of H-bonded complexes of variously substituted aniline and anilinium cation derivatives with various oxygen and nitrogen acids/bases were retrieved from CSD[31] with the following restrictions: (1) the searches were performed for substituted aniline (anilinium cation) interacting with a nitrogen or oxygen base/acid (base) with an intermolecular contact between the nitrogen of aniline (anilinium cation) and the nearest O or N atom in the base/acid (base) equal to or less than the sum of their van der Waals radii;[33] (2) the searches were restricted to structure measurements with the reported mean estimated standard deviation of the C−C bond ≤ 0.005 Å, not disordered and with an *R* factor < 0.05. The data were retrieved for the mono- and polysubstituted aniline/anilinium cation (by any of the following substituents: halogen, −Me, −CN, −COOH, $-COO^-$, −COOMe, −COOEt, $-CONH_2$, $-CF_3$, $-NH_2$, $-NH_3^+$, $-NO_2$, −OH, −OMe, $-SO_3^-$, or −H) interacting with the N or O atom in the acid/base partner. Sometimes, solvent molecules were also present in the crystal lattice.

Ab initio modeling, which is equivalent to gas-phase measured properties, was applied to the aniline, anilide anion, and anilinium cation derivatives substituted in position 4 (X = NO, NO_2, CN, CHO, H, CH_3, OCH_3, and OH) and their H-bonded complexes (only for X = NO, NO_2, CHO, H, and OH) with B (B═F^-, CN^-) or HB (HB = HF, HCN), see Chart 1. In H-bonded complexes, the linearity of N···H···B was assumed.[32]

Becke-style three-parameter density functional theory using the Lee−Yang−Parr correlation functional[34] and 6-311+G** basis set[35] (B3LYP/6-311+G**) and the second-order Moller−Plesset perturbation method[36] with the Dunning basis set[37] aug-cc-pVDZ (MP2/aug-cc-pVDZ) were used to optimize the geometries of the molecules and complexes, and also to calculate vibrational frequencies. The absence of imaginary frequencies verified that all structures were true minima. In the text below, abbreviations B3LYP and MP2 were applied. In the cases of aniline and substituted anilines,

Chart 2[a]

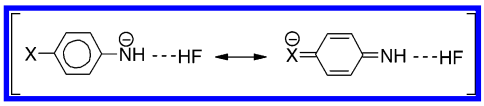

[a] X = NO, NO_2, CHO

B3LYP was found as very accurate in predicting the structural properties[38,39] and vibrational spectra.[39] Two methods of computation were used since the MP2 procedure covers the dispersion energy, which might play an important role in stabilizing molecular clusters.

NICS estimated in the center of the ring,[18] NICS, and 1 Å above the center of the ring,[19] NICS(1), were calculated at the HF/6-31+G* level of theory using the gauge invariant atomic orbital method. Additionally, the perpendicular to the molecular plane component of the tensor,[20,40] $NICS(1)_{zz}$, was also estimated.

All calculations were performed using the Gaussian 03 series of programs.[41]

Geometry parameters of the ring (CC bond lengths) were used to calculate aromaticity index HOMA,[17,42] which reads

$$\mathrm{HOMA} = 1 - \frac{\alpha}{n}\sum (R_{\mathrm{opt}} - R_i)^2 \qquad (1)$$

where *n* is the number of bonds taken into the summation, α is a normalization constant (for CC bonds α = 257.7) fixed to give HOMA = 0 for a model nonaromatic system, for example, the Kekulé structure of benzene,[43] and HOMA = 1 for the system with all bonds equal to the optimal value R_{opt} assumed to be realized for fully aromatic systems (for CC bonds R_{opt} is equal to 1.388 Å), and R_i stands for the running bond length.

H-bonding energy, *E*, is the sum of two terms:[32] interaction energy, E_{int}, and deformation energy (due to the geometry change of the molecules caused by the interaction). E_{int} was computed by use of the formula[32]

$$E_{\mathrm{int}} = E_{\mathrm{AB}}(\mathrm{basis}_{\mathrm{AB}};\mathrm{opt}_{\mathrm{AB}}) - E_{\mathrm{A}}(\mathrm{basis}_{\mathrm{AB}};\mathrm{opt}_{\mathrm{AB}}) - E_{\mathrm{B}}(\mathrm{basis}_{\mathrm{AB}};\mathrm{opt}_{\mathrm{AB}}) \qquad (2)$$

where A is aniline or a related derivative (anilide anion) and B is F^- (or HF, see Chart 1). $E_{\mathrm{A}}(\mathrm{basis}_{\mathrm{AB}};\mathrm{opt}_{\mathrm{AB}})$ means the energy of molecule A, E_{A}, in the H-bonded AB system basis set, $\mathrm{basis}_{\mathrm{AB}}$, for its geometry in the optimized complex AB, $\mathrm{opt}_{\mathrm{AB}}$. The other terms of the equation should be understood in the same way.

The gas-phase acidity, $\Delta_{\mathrm{acid}}G$, and enthalpy of acidity (proton affinity), $\Delta_{\mathrm{acid}}H$, of para-substituted aniline and anilinium cation derivatives and hydrofluoric and hydrocyanic acids were obtained[44,45] as the Gibbs energy and enthalpy changes of the reaction:

$$\mathrm{HA} \rightleftarrows \mathrm{A}^- + \mathrm{H}^+ \qquad (3)$$

No scaling was applied to obtained frequencies for the calculation of thermodynamic parameters, which were temperature-corrected to 298 K. In the case of H^+, the only nonzero energy term is the translational one, which is equal to $^3/_2RT$; therefore, $H(H^+) = {}^5/_2RT$ ($H = E + PV$, $PV = RT$, for 298 K $H(H^+)$ = 1.48 kcal/mol). We used the Sackur−Tetrode equation to evaluate the entropy of the proton,[45] $TS(H^+)$ = 7.76 kcal/mol at 298 K and 1 atm pressure, which

Table 1. Experimental and Calculated (B3LYP/6-311+G** and MP2/aug-cc-pVDZ) Gas-Phase Acidity, $\Delta_{acid}G_{298}$, and the Proton Affinity of the Anion, $\Delta_{acid}H_{298}$, at 298 K for Reaction 3

		$\Delta_{acid}G_{298}$/kcal/mol			$\Delta_{acid}H_{298}$/kcal/mol		
		exptl.	B3LYP	MP2	exptl.	B3LYP	MP2
4-NO	$C_6H_4NH_2$		333.1	331.8		340.2	338.9
4-NO_2	$C_6H_4NH_2$	336.2[a]	333.3	333.3	343.5[a]	340.4	340.3
4-CN	$C_6H_4NH_2$	341.5[a]	340.5	338.7	348.8[a]	347.9	346.1
4-CHO	$C_6H_4NH_2$	342.3[a]	340.4	338.6	349.6[a]	347.6	345.8
4-H	$C_6H_4NH_2$	359.1[b]	359.4	355.6	366.4[b]	366.8	363.0
4-CH_3	$C_6H_4NH_2$	360.1[b]	360.9	355.5	367.3[b]	368.0	364.8
4-OCH_3	$C_6H_4NH_2$	359.8[b]	360.0	356.4	367.1[b]	367.9	364.1
4-OH	$C_6H_4NH_2$		360.9	357.2		368.8	365.3
4-NO	$C_6H_4NH_3^+$		189.1	192.1		197.0	198.8
4-NO_2	$C_6H_4NH_3^+$	199.4[c]	188.4	190.3	207.0[c]	194.8	197.1
4-CN	$C_6H_4NH_3^+$		189.9	191.0		198.0	197.9
4-CHO	$C_6H_4NH_3^+$		195.8	194.5		200.6	201.4
4-H	$C_6H_4NH_3^+$	203.3[c]	203.3	201.5	209.1[d]	209.8	208.5
4-CH_3	$C_6H_4NH_3^+$	206.7[c]	204.9	203.2	214.3[c]	213.3	211.5
4-OCH_3	$C_6H_4NH_3^+$	207.6[c]	208.1	205.3	215.2[c]	214.9	212.6
4-OH	$C_6H_4NH_3^+$		205.8	203.4		212.9	210.7
	HF	365.5[e]	361.8	359.4	371.3[e]	367.6	365.2
	HCN	343.6[f]	339.9	338.2	350.9[f]	350.2	348.4

[a] Experimental data taken from NIST Chemistry WebBook[52] after Taft and Topsom.[49] [b] Experimental data taken from NIST Chemistry WebBook[52] after Bartmess et al.[53] [c] Experimental data taken from NIST Chemistry WebBook[52] after Hunter and Lias.[56] [d] Experimental data taken from NIST Chemistry WebBook[52] after Hillebrand et al.[57] [e] Experimental data taken from NIST Chemistry WebBook[52] after Blondel et al.[54] [f] Experimental data taken from NIST Chemistry WebBook[52] after Bradforth et al.[55]

gives a value for $G(H^+)$ of −6.28 kcal/mol ($G = H - TS$). Calculations were carried out at the B3LYP and MP2 levels. The basis set superposition error[46] (counterpoise correction) for the above reaction was equal to or less than 0.4 kcal/mol (B3LYP), so it was neglected.

RESULTS AND DISCUSSION

Our analysis is based both on structural data from experimental X-ray diffraction[31] and on the data from ab initio optimization. In the latter case, the gas-phase acid/base properties of chemical systems in question are often dramatically different from our knowledge from aqueous solution.[47] It is noteworthy to say that in the gas phase HF is a weaker acid than p-substituted aniline (in the case of aniline by ∼5 kcal/mol[48]), whereas HCN is a stronger acid than aniline[48] but weaker than, for example, 4-formylaniline[49] (see Table 1). The acidity of HF leads to an obvious consequence that in the case of complexes with anilines the favorable structure should be $X-C_6H_4-NH^-\cdots HF$. These expectations resulting from gas-phase basicity/acidity equilibria are not always supported by our modeling computation.

If neutral p-substituted aniline derivatives are considered to be acting as bases with neutral acids (HB = HF, HCN), then due to the much lower basicity of the NH_2 group than that of F^- and CN^- in the gas phase, they form H-bonded complexes without proton transfer, that is, $X-C_6H_4-NH_2\cdot\cdot\cdot HB$. It is in line with a general rule[24b] that the reactions with charge separation are not privileged in the gas phase, in opposition to these reactions carried out in the polar media, and with the Alkorta et al.[50] model. Their model[50] allows to predict when a hydrogen-bonded cluster between the corresponding neutrals (base and acid) would be stable or a spontaneous proton transfer from acid toward base should be observed.

Four kinds of H-bonded complexes were defined and considered in this report, both based on X-ray diffraction data and ab initio optimization: (i) $NH_3^+\cdots B$ interactions for anilinium cation derivatives acting as acids [Chart 1 (i)]; (ii) $NH_2\cdots HB$ interactions for aniline derivatives acting as bases [Chart 1 (ii)]; (iii) $NH_2\cdots B$ interactions for aniline derivatives acting as acids [Chart 1 (iii)]; and (iv) $NH^-\cdots HB$ interactions for anilide anion derivatives acting as bases [Chart 1 (iv)].

Analysis of the data from crystalline phases is somewhat biased by numerous intermolecular interactions (by so-called crystal packing forces[51]), and hence the dependences between structural parameters may exhibit a substantial scatter.

Computational Modeling of H-Bonding of p-Substituted Aniline, Anilide Anion, and Anilinium Cation Derivatives. In order to check reliability of the computational data used in our analysis, we have made a comparison of the calculated and experimental values of gas-phase acidity[52] presented in Table 1. The reaction used for the estimation of $\Delta_{acid}G_{298}$ and $\Delta_{acid}H_{298}$ reads as eq 3.

It results from the above comparison that the differences between the experimental data[52,57] and those computed at the B3LYP level of theory used in our analyses are practically meaningless. Moreover, gas-phase acidity and proton affinity values computed at a higher level of theory, MP2, are lower than the experimental data, and in a large majority of cases, they are lower than calculated at the B3LYP level. A recent paper[58] presents proton affinities of anionic bases. Swart and Bickelhaupt[58] compare results for four different quantum chemical approaches: BP86/TZ2P, BP86/QZ4P//BP86/TZ2P, B3LYP/aug-cc-pVTZ,[59] and CCSD(T)/aug-cc-pVQZ//B3LYP/aug-cc-pVTZ.[59] The comparison led them to the conclusion that the best of these methods (BP86/QZ4P//BP86/TZ2P), applied to 17 mostly simple organic bases, gives a mean absolute deviation equal to 1.6 kcal/mol for the proton affinity at 0 K with respect to high-level ab initio benchmark data. For a base most similar to ours (as far as the size is concerned), $C_6H_5^-$, the best agreement was for B3LYP/aug-cc-pVTZ (399.9 kcal/mol comparing to an experimental value of 399.6 kcal/mol). All

Chart 3

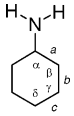

other, more advanced methods presented in the paper[58] gave greater differences. Their data for HF and HCN at 0 K are 367.1 and 348.8 kcal/mol;[58] thermal correction[59] to 298 K gives 367.4 and 349.6 kcal/mol, whereas our B3LYP data are 367.6 and 350.2 kcal/mol (MP2 results: 365.2 and 348.4 kcal/mol), respectively. In the case of the proton affinity of the anilinium cation, the calculated value (209.8 kcal/mol, B3LYP) is in the range of experimental ones (210.9 and 209.1 kcal/mol)[56,57] and is almost equal (209.5 kcal/mol) to that obtained by the MP2/6-311+G**//HF/6-31G* theoretical model.[57] Ervin and DeTuri[59] have found that the theoretical calculation of gas-phase acidities at the CCSD(T)/aug-cc-pVTZ//B3LYP/aug-cc-pVTZ level provides excellent matches with experimental values. Other computational methods (DFT and MP2) give reasonable results for acidities, as was stated in previous comparisons of experimental and theoretical gas-phase acidities.[45c,60]

Additionally, the B3LYP and MP2 computed values of the hydrogen-bond energy (counterpoise correction was taken into account, see Supporting Information) for $C_6H_5NH_2\cdots F^- \rightarrow C_6H_5NH_2 + F^-$ at 298 K are 33.0 and 31.9 kcal/mol, respectively, whereas the experimental[48,52] value is 31.2 (±2.0) kcal/mol. Thus, it seems that the level of theory used is reliable.

It should be pointed out that the structural entities depicted in Chart 1 may result for having the fluoride anion as a base, B, from equilibria 4 and 5.

$$4\text{-X-}C_6H_4NH_3^+ + F^- \rightleftarrows 4\text{-X-}C_6H_4NH_2 + HF \quad (4)$$

$$4\text{-X-}C_6H_4NH_2 + F^- \rightleftarrows 4\text{-X-}C_6H_4NH^- + HF \quad (5)$$

In the gas phase, that is, in the state modeled by quantum chemical optimizations (in our case $B = F^-$ or CN^-), the position of equilibrium depends on the proton affinities of B and 4-X-$C_6H_4NH_2$ in eq 4 and B and 4-X-$C_6H_4NH^-$ in eq 5. These kinds of equilibria may be associated with more detailed ones, such as those presented in a general way (eq 6) by Alkorta et al.[50]

$$\text{A-H} + \text{base (6a)} \rightleftarrows \text{A-H}\cdots\text{base (6b)} \rightleftarrows A^-\cdots Hbase^+ \text{ (6c)} \rightleftarrows A^- + Hbase^+ \text{(6d)} \quad (6)$$

where A-H is a neutral acid and base is a neutral base, and the concentrations of each of the states in equilibria 6 depend on the energy of each of them following the Boltzmann distribution low. Thus, even if the equilibrium in 6a ⇔ 6b is pushed significantly in one of the probable directions, the other states still exist in some little concentration.[61] As such, they are realized by some chemical entities with their own structure and properties. Therefore, in our investigations, we have taken into consideration both systems like 6b and 6c, despite the fact that their concentration in equilibrium may be very small. Hence, all four H-bonded complexes i−iv in Chart 1 are subjects of the structural study in this paper.

Two classes of structural data have been analyzed: first, the aniline, its 4-substituted derivatives, their anilinium cations and anilide anions—all of them may serve as reference systems without H-bond interactions—and, second, the systems involved in H-bond complexation. There are aniline and its 4-substituted derivatives as well as their anilide complexes with fluoride/hydrofluoric acid and cyanide/hydrocyanic acid interacting with the nitrogen via H-bonding in their optimal geometry, that is, in an equilibrium state. Tables S1 and S2 (Supporting Information) present geometrical parameters of the ring and C−N bond lengths, whereas Table 2 presents aromaticity indices HOMA and NICSs values and interatomic distances between the donor and acceptor for H-bonded systems. For the complexes of 4-nitroso, 4-nitro and 4-formylo derivatives of aniline with F^- in the optimal geometry (both B3LYP and MP2), the proton is located at fluoride [Chart 1(iv)]; thus, the complex has a form as shown in Chart 2. The negative charge at the nitrogen is then mesomerically delocalized over the ring, leading to a quinoid structure.

NH_3^+, NH_2, and NH^- groups involved in H-bonding with bases ($B = F^-$ or CN^-) or acids (HB = HF or HCN) change their electronegativities. For NH_3^+ and NH_2, the Domenicano electronegativities[10] are 4.31 and 2.63, respectively. By analogy with the OH and O^- pair (electronegativities of them are 3.21 and 0.98, respectively),[10] for the NH_2 and NH^- pair, one can expect values of 2.63 and around 0.5−1.0, respectively. Undoubtedly, if NH_3^+, NH_2, or NH^- are involved in H-bonding, then the electronegativities of these groups should change similarly as it was found for OH/O^- groups in phenols involved in H-bonding.[62] As a result of these changes, two kinds of structural consequences are observed and have to be considered. First the changes in vicinity of the H-bonding region are discussed—the interrelations between the C−N and *a* bond lengths and α angle; then, the more distant consequences—the changes in geometry and π-electron delocalization in the ring—will be discussed.

Figures 1 and S1 present typical Bent−Walsh[63] interrelations between the *a* and the C−N bond lengths and α angle. For labeling, see Chart 3.

Apart from the typical effect due to the changing electronegativity of the group involved in H-bonding[62] and hence Bent−Walsh[63] interrelations between bond lengths C−N and *a*, and valence angle α (Chart 3), an important contribution may stem from the mesomeric effect. This is particularly important for electron-accepting substituents which interact via the through-resonance effect with electron-donating nitrogen involved in H-bonding: $NH_2\cdots B$ and $NH_2\cdots HB$. In both cases, the electronic status of the nitrogen atom is modified due to H-bonding. This modification may be enhanced or diminished by the resonance effect. Interestingly, the C−N bond length versus the α angle is close to being linear with an acceptable good correlation, cc = 0.94. Two other relationships are slightly curved. In the case of the *a* versus C−N bond length scatter plot, the curvature might be interpreted as being a result of less energy needed for the deformation of a single bond (*a* bonds) than for that of a double (partly) bond (C−N). The force constants for stretching single and double bonds are roughly in a 1:2 ratio.[64] The scatter for the relations in subgroups (described in Figures 1 and S1 as $NH_2\cdots HB$, $NH_2\cdots B$, and $NH^-\cdots HF$ systems of interactions and aniline, anilinium, and anilide derivatives), in cases of α versus d_{CN} and *a* versus α, may

Table 2. C−N Bond Lengths, d_{CN}, and Aromaticity Indices HOMA and NICSs Values for (a) 4-X-Aniline, 4-X-Anilide Anion, and 4-X-Anilinium Cation (X = NO, NO_2, CN, CHO, H, CH_3, OCH_3, and OH) and (b) Their H-Bonded Complexes (only for X = NO, NO_2, CHO, H, and OH; Interatomic Distances between Heavy Atoms in the Hydrogen Bond, $d_{N\cdots B}$, Included). B3LYP Results

Part a

X		d_{CN} /Å	HOMA	NICS	NICS(1)	$NICS(1)_{zz}$
NO	NH_2	1.374	0.922	−8.39	−9.55	−23.92
NO_2	NH_2	1.378	0.956	−9.89	−10.14	−24.72
CN	NH_2	1.383	0.947	−9.91	−10.40	−26.24
CHO	NH_2	1.382	0.941	−8.95	−10.09	−25.50
H	NH_2	1.398	0.976	−9.77	−10.72	−28.55
CH_3	NH_2	1.401	0.975	−10.00	−10.73	−28.12
OCH_3	NH_2	1.407	0.976	−11.37	−11.04	−28.20
OH	NH_2	1.406	0.982	−11.43	−10.97	−27.95
NO	NH^-	1.314	0.399	−0.19	−3.44	−6.80
NO_2	NH^-	1.315	0.497	−2.11	−4.03	−7.56
CN	NH^-	1.320	0.527	−3.54	−4.77	−11.16
CHO	NH^-	1.318	0.472	−1.92	−4.25	−9.71
H	NH^-	1.332	0.670	−4.19	−5.64	−15.75
CH_3	NH^-	1.334	0.686	−4.76	−5.89	−15.89
OCH_3	NH^-	1.334	0.693	−6.27	−6.28	−15.52
OH	NH^-	1.335	0.704	−6.36	−6.51	−16.31
NO	NH_3^+	1.497	0.993	−11.76	−11.55	−29.91
NO_2	NH_3^+	1.496	0.999	−12.54	−11.97	−30.21
CN	NH_3^+	1.496	0.982	−11.85	−11.86	−30.26
CHO	NH_3^+	1.497	0.988	−11.35	−11.76	−30.16
H	NH_3^+	1.498	0.994	−11.21	−11.75	−31.35
CH_3	NH_3^+	1.497	0.983	−11.16	−11.53	−29.95
OCH_3	NH_3^+	1.494	0.966	−11.69	−11.17	−28.22
OH	NH_3^+	1.494	0.981	−11.72	−11.06	−28.23

Part b

	X	$d_{N\cdots B}$ /Å	d_{CN} /Å	HOMA	NICS	NICS(1)	$NICS(1)_{zz}$
$NH^-\cdots HF$[a]	NO	2.471	1.323	0.576	−2.42	−5.18	−11.47
$NH_2\cdots CN^-$	NO	2.890	1.339	0.776	−5.60	−7.56	−18.00
$NH^-\cdots HF$[a]	NO_2	2.468	1.324	0.664	−4.40	−5.83	−12.39
$NH_2\cdots CN^-$	NO_2	2.895	1.341	0.842	−7.53	−8.24	−19.03
$NH^-\cdots HF$[a]	CHO	2.449	1.328	0.654	−4.22	−6.19	−14.79
$NH_2\cdots CN^-$	CHO	2.929	1.345	0.829	−6.97	−8.42	−20.70
$NH_2\cdots F^-$	H	2.450	1.349	0.867	−7.47	−8.66	−23.20
$NH_2\cdots CN^-$	H	3.030	1.370	0.934	−8.89	−9.99	−26.44
$NH_2\cdots F^-$	OH	2.476	1.360	0.911	−10.08	−9.79	−24.75
$NH_2\cdots CN^-$	OH	3.052	1.381	0.956	−11.01	−10.64	−26.83
$NH_2\cdots HF$	NO	2.713	1.412	0.965	−9.66	−10.51	−26.75
$NH_2\cdots HCN$	NO	3.330	1.398	0.951	−9.26	−10.22	−25.95
$NH_2\cdots HF$	NO_2	2.710	1.414	0.984	−10.91	−10.99	−27.25
$NH_2\cdots HCN$	NO_2	3.317	1.400	0.975	−10.57	−10.74	−26.49
$NH_2\cdots HF$	CHO	2.700	1.417	0.971	−9.85	−10.87	−27.73
$NH_2\cdots HCN$	CHO	3.297	1.404	0.961	−9.54	−10.66	−27.10
$NH_2\cdots HF$	H	2.671	1.428	0.989	−10.31	−11.18	−29.91
$NH_2\cdots HCN$	H	3.223	1.417	0.984	−10.08	−11.01	−29.54
$NH_2\cdots HF$	OH	2.657	1.433	0.990	−11.69	−11.18	−28.68
$NH_2\cdots HCN$	OH	3.204	1.423	0.987	−11.55	−11.10	−28.52

[a] In this case, the quinoid canonical structure (Chart 2) is dominant.

be interpreted as the result of a substituent effect (mostly mesomeric), whereas the main direction of the regressions for these two cases is associated with changes in electronegativity of the amine and related groups due to H-bond formation.

In order to quantify the H-bond formation energy (eq 2) in terms of the structural parameter, d_{CN}, the plot of E_{int} versus d_{CN} is shown in Figure 2 (data, including BSSE, in Table S3 of the Supporting Information), following a procedure published elsewere.[32] For interactions in which the NH_2 group is proton-donating (i.e., $NH_2\cdots B$ interactions, B = F^-), the dependence has a positive slope. The stronger the H-bond is, the shorter the C−N bond is. There is a full analogy with a similar situation in cases of H-bond formation of phenol derivatives with bases.[30,32] However, for $NH_2\cdots$HB and $NH^-\cdots$HB (HB = HF) interactions, both regressions have negative slopes. There is a simple interpretation: the formation of $NH_2\cdots B$ bonding is associated with an increase of lone-pair mobility. The more distant the proton is from the nitrogen atom, the more mobile the lone pair; hence, the shortening of the C−N bond may be observed. If, in the para position, an electron-accepting substituent is attached, then due to its attraction power the shortening may be enhanced. The stronger the H-bond is, the more mobile the electron pair is and the stronger the mesomeric effect may be. The situation for cases $NH^-\cdots$HB and $NH_2\cdots$HB is opposite. In both cases, an increase of H-bond energy (as absolute value) is associated with an immobilization of the lone pair because it becomes a partner for H-bond formation. This generates a lesser opportunity to interact mesomerically

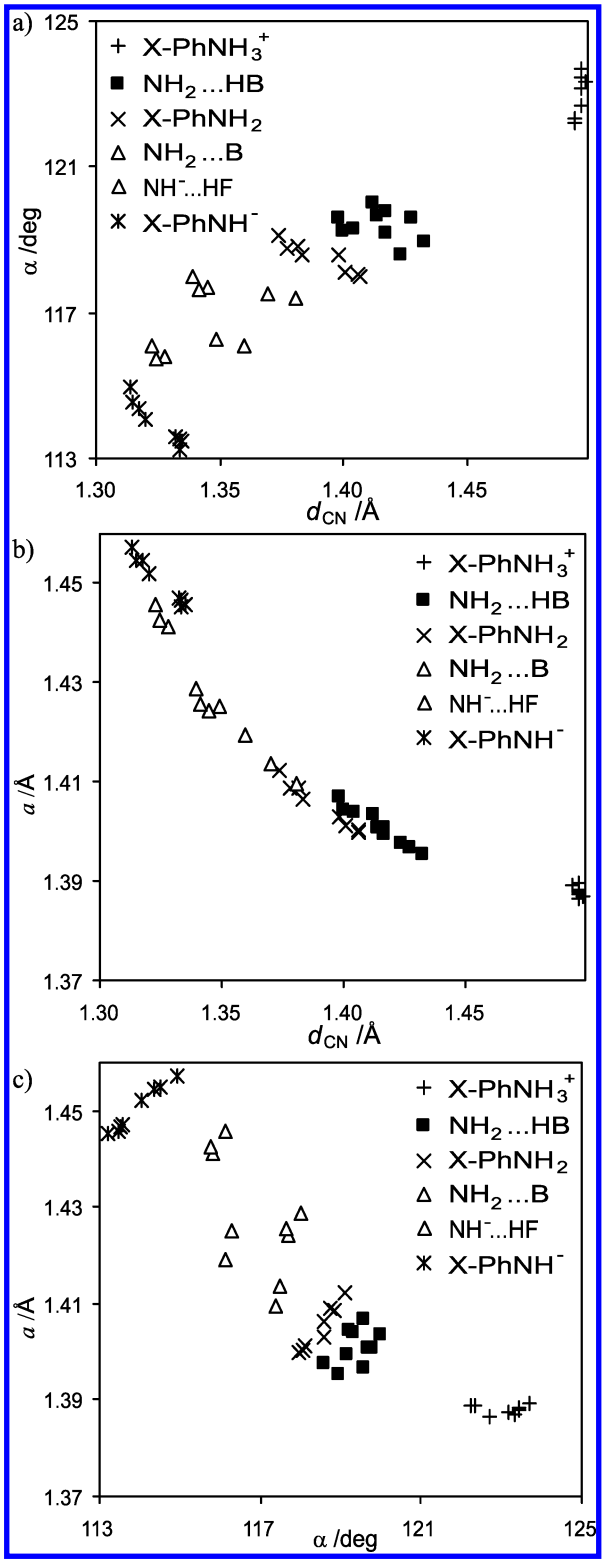

Figure 1. Interrelations between (a) α and C−N bond length, d_{CN}; (b) *a* and C−N bond length; (c) *a* bond length and α for B3LYP optimized geometry of 4-substituted aniline, anilide anion, and anilinium cation and their H-bonded complexes. Ph means C_6H_4.

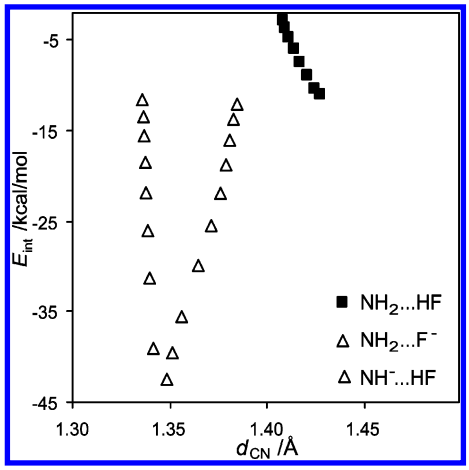

Figure 2. Dependence of the H-bond interaction energy, E_{int}, on C−N bond length, d_{CN}, for the B3LYP modeling interaction of aniline as $NH_2\cdots HF$, $NH_2\cdots F^-$, and $NH^-\cdots HF$ systems.

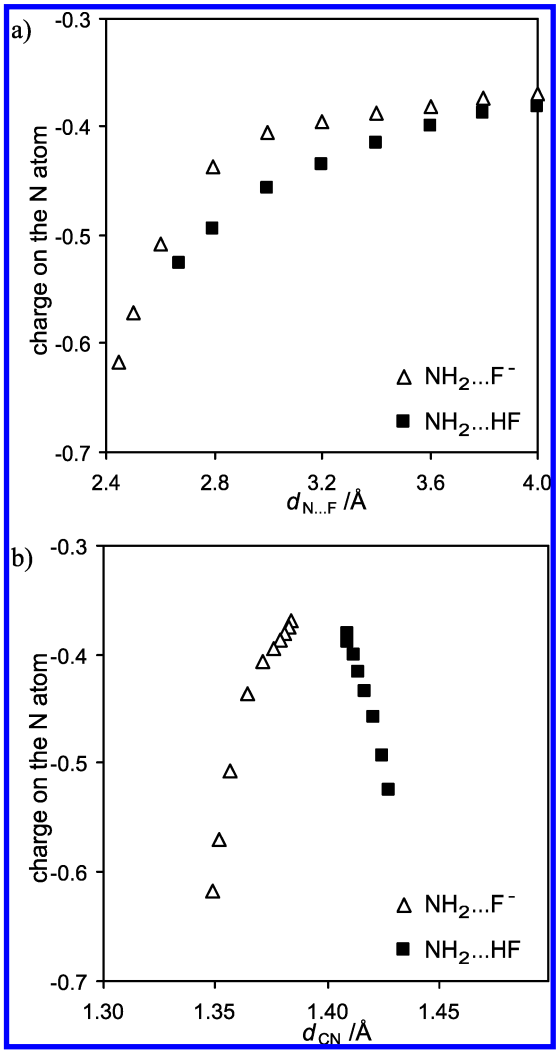

Figure 3. Dependence of the Mulliken charges at the nitrogen atom on the (a) N···F interatomic distance, $d_{N\cdots F}$, and (b) C−N bond length, d_{CN}, for the B3LYP modeling interaction of $C_6H_5NH_2$ as $NH_2\cdots F^-$ and $NH_2\cdots HF$ systems.

with electron-attracting substituents in the para position in the ring and, as a consequence, smaller changes in the C−N bond length. Thus, the C−N bond length may be used as a reliable parameter describing the mobility of the lone pair at the nitrogen atom in groups NH_2 and NH^- involved in H-bond complexation. An increase of this mobility is associated with an increase of the strength of $NH_2\cdots B$ interactions and with a decrease of $NH_2\cdots HB$ interactions.

The above reasoning is supported by dependences presented in Figure 3. Moving B (B = F) to the nitrogen atom[32] [Chart 1 (ii and iii)] leads in both cases ($NH_2\cdots F^-$ and $NH_2\cdot$

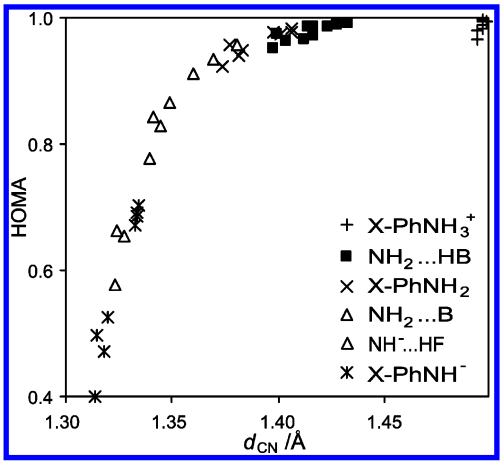

Figure 4. Scatter plot of HOMA vs C−N bond length, d_{CN}, for the B3LYP optimized geometry of 4-substituted aniline, the anilide anion, and the anilinium cation and their H-bonded complexes. Ph means C_6H_4.

··HF) to an increase of electron charge (Mulliken charges[65]) at the nitrogen. This however acts on the C−N bond length, and the relation between the C−N bond length and the electron charge at the nitrogen atom is different for $NH_2\cdots F^-$ and $NH_2\cdots HF$ interactions, as argued earlier.

Changes in interactions in the H-bond region lead to substantial changes in the geometry of the ring in the above-mentioned systems. Application of the HOMA index to the optimized geometries of model systems (Table 2) has led to scatter plots as shown in Figure 4.

This is a similar observation to that found for phenol/phenolate systems analyzed for experimental and theoretically optimized geometries.[14−16] Note that the greatest changes in aromaticity index HOMA are found for two cases: for $NH_2\cdots B$ and $NH^-\cdots HB$ interactions. In the first case, H-bonding enhances the mobility of the lone pair at the nitrogen atom and allows an increase of the mesomeric effect, which in turn increases the contribution of the quinoid structure, that is, leads to a decrease of cyclic π-electron delocalization. In another case, the lone pair at the nitrogen atom NH^- group may be involved in strong mesomeric interactions with a substituent with attracting power. These interactions have to be decreased if the lone pair is involved in H-bonding with a Broensted acid HB.

Application of magnetism-based aromaticity indices NICS,[18] NICS(1),[19] and NICS(1)$_{zz}$[20] (for a review, see Chen et al.[4g]) has led to a picture equivalent to that found for HOMA. Figure 5 presents the dependences of NICSs (Table 2) on the C−N bond length. The shorter the C−N bond is, the stronger is the decrease of the aromatic character of the ring in aniline/anilide/anilinium H-bonded complexes. The relationships may be approximated by curves which change in a monotonic way. The most regular curves are for the dependences of NICS(1) and NICS(1)$_{zz}$ on the C−N bond length.

Once again, the equivalence of aromaticity indices HOMA and NICSs is shown for systems with homogeneous changes in structure.[11,14] Figure 6 presents the dependence of NICS(1) and NICS(1)$_{zz}$ on HOMA. Interestingly, a weak curvature observed for the most aromatic rings (HOMA close to 1.0) allows one to suggest that NICS(1) and NICS(1)$_{zz}$ are more sensitive parameters than HOMA for the description of π-electron delocalization. Again, good mutual relationships

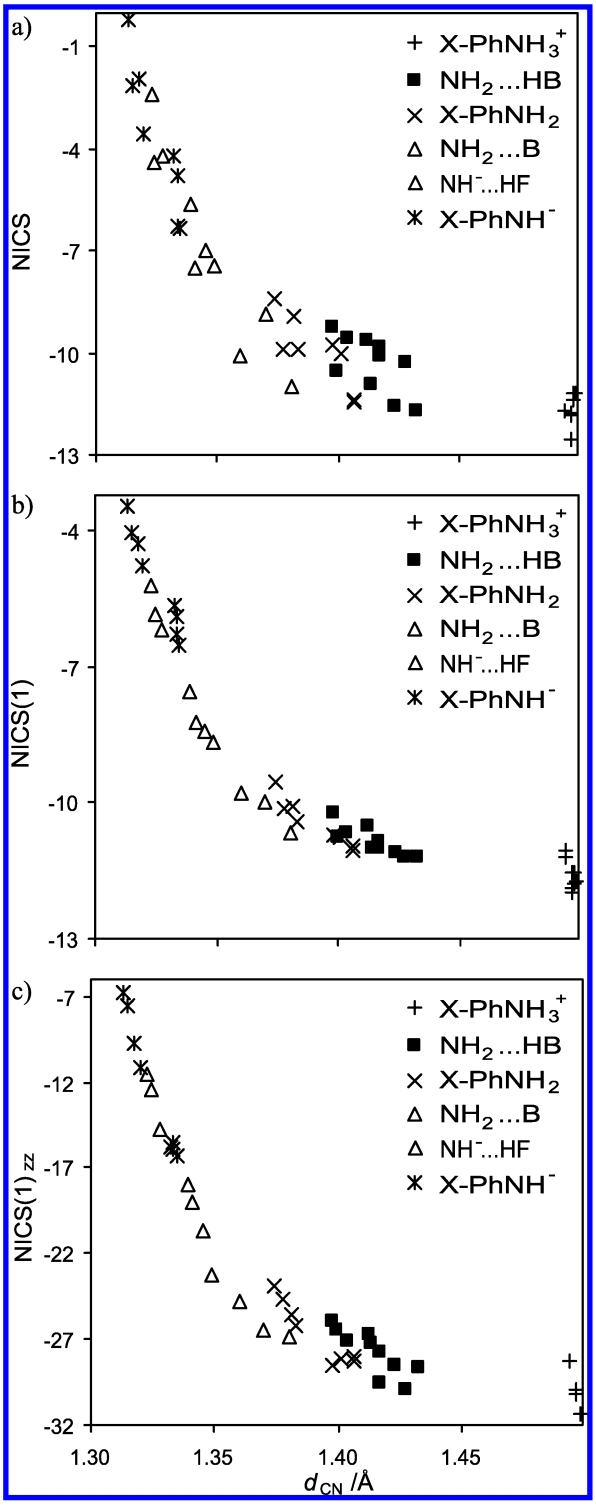

Figure 5. Dependences of (a) NICS, (b) NICS(1), and (c) NICS(1)$_{zz}$ on C−N bond length, d_{CN}, for the B3LYP optimized geometry of 4-substituted aniline, the anilide anion, and the anilinium cation and their H-bonded complexes. Ph means C_6H_4.

between those two different aromaticity indices support our earlier statement[66] that, for systems with similar perturbation in the structure, the indices follow some kind of a collinear or at least regular, monotonic relationship.

Analysis of X-ray Structural Data. Analysis of experimental geometries of variously substituted derivatives of the aniline and anilinium cation (anilide anion derivatives with H-bonding are not known crystallographically) leads to results which are qualitatively in agreement with those

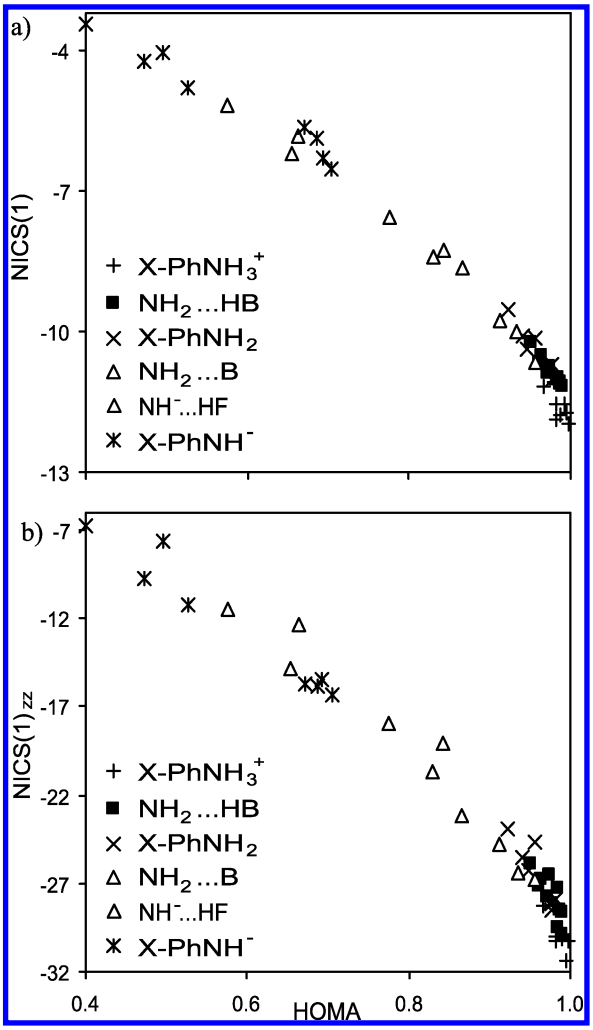

Figure 6. Dependence of (a) NICS(1) and (b) $NICS(1)_{zz}$ on HOMA for the B3LYP optimized geometry of 4-substituted aniline, the anilide anion, and the anilinium cation and their H-bonded complexes. Ph means C_6H_4.

obtained by quantum chemical modeling. The interrelations between the C−N and *a* bond lengths and α angle are shown in Figure 7. It should be pointed out that all the data presented in Figure 7 are for mono- and polysubstituted species. These substituents may be involved in intramolecular interactions which may contribute to deformations of the ring geometry. Dispersion of the data from ab initio optimization (Figures 1 and S1) is in general smaller than that observed for experimental scatter plots (Figure 7), but for both experiments, in the solid state and optimized data, observed variabilities of the geometric parameters are alike.

It results from Figure 7 that for all presented relationships statistically significant[67] (for details, see the Supporting Information, Table S4) linear dependences exist for all data points. The worst (cc = −0.75), but still statistically significant, is the correlation between *a*-bond length and α angle, shown in Figure 7c. This means that as a whole set of data they follow a general rule—the Bent−Walsh rule.[63] The rule relates an increase (or a decrease) of electronegativity of the substituent Y (in our case, the functional group NH_2 involved in H-bonding, Scheme 1) with an increase (or a decrease) of the 2p orbital contribution to the sp^2 hybridized carbon atom directed to Y and a decrease (or an increase) of this contribution to bond orbitals in the two other

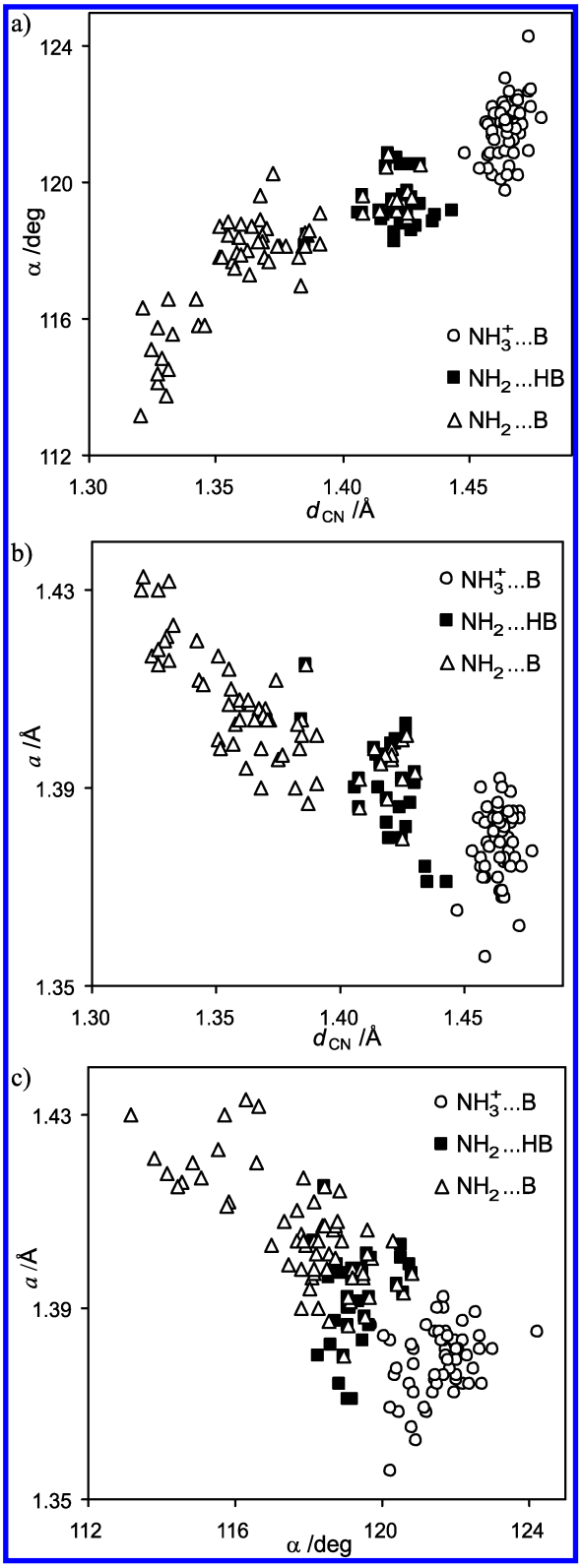

Figure 7. Dependence of the (a) α angle on C−N bond length, d_{CN}, (b) *a* on C−N bond length, d_{CN}, and (c) *a* bond length on the α angle for variously substituted aniline/anilinium cation derivatives in their H-bonded complexes (experimental data retrieved from CSD); for all data, $n = 332$, correlation coefficients are cc = 0.91, −0.86, and −0.75, respectively.

directions (ortho−ipso CC bonds).[8a,29] This in turn results in a lengthening (or shortening) of the C−Y bond, a shortening (or lengthening) of both ipso−ortho CC bonds, and an increase (or a decrease) of the ipso bond angle.

Scheme 1. Changes in Hybridization at the Carbon Atom as a Result of Changes in Electronegativity of the Nitrogen Atom in the Aniline Molecule Involved in Two Kinds of H Bonding

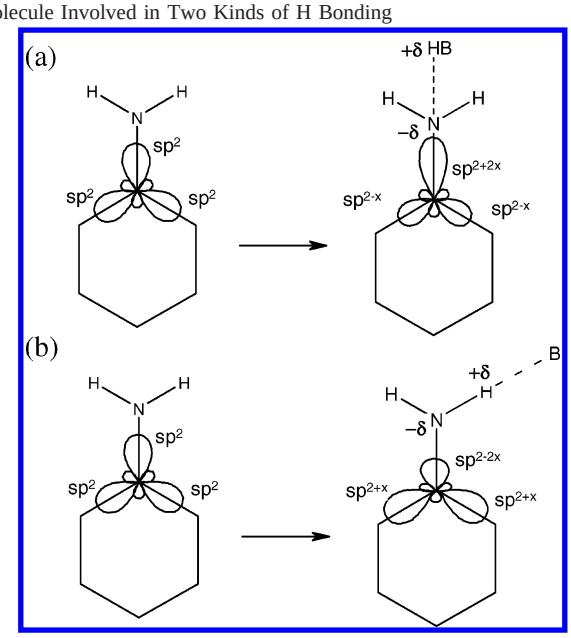

Scheme 1 shows how this rule works in the case of aniline involved in H-bonding. A contribution of the mesomeric effect cannot be excluded, but there is no clear relation between the C−N bond length and α angle for these kinds of interactions.

The following conclusion may be postulated now: the $-NH_2$ group in substituted aniline derivatives may act either as a Lewis acid interacting with appropriate bases or as a Lewis base interacting with H-acids, and these two kinds of interactions lead to different structural consequences.

Finally, it is observed that the C−N bond length varies within a narrow range for the case where N−H in anilinium derivatives (case i) is involved in H-bonding with bases. The $-NH_3^+$ group is rather strongly acidic, and as long as a proton is not transferred to the base B ($C_6H_5NH_3^+\cdots B \rightarrow C_6H_5NH_2 + HB^+$), the nitrogen atom has neither a mobile nor polarizable lone pair. However, changes in hyperconjugation[68] in the NH_3^+ group due to H-bonding interactions have to be taken into account. As a consequence, there is a faint possibility of mesomeric effects that are associated with the shortening of the C−N bond.

Figure 8 presents the dependence of C−N bond length on N···O(N) interatomic distance, a quantity often used as an approximate measure of H-bonding strength.[27d,69] The figure shows that C−N bond length practically does not depend on the N···O(N) interatomic distance for the $NH_3^+\cdots B$ interaction (case i), but some dispersion in d_{CN} exists. In both other cases, where either the nitrogen atom is proton-accepting (case ii) or the N−H bond is proton-donating (case iii), the dispersion is much wider; the scatter plots represent broad clusters, indicating, for case ii, a roughly negative slope. They show large variations of C−N bond lengths with changes of the N···O(N) interatomic distance for systems with $NH_2\cdots B$ and $NH_2\cdots HB$ interactions, but in a chaotic way. Roughly, it may be said that C−N bond length for i does not depend on H-bond strength, and clusters for ii and iii exhibit a substantial dispersion and are separated. This is documented by mean values of the C−N bond length of 1.465, 1.420, and 1.371 Å, with estimated standard deviations

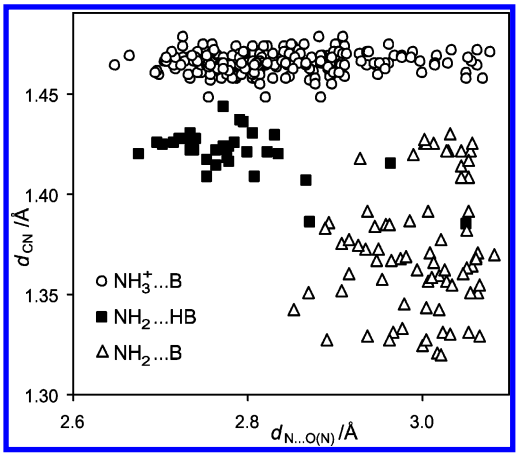

Figure 8. Dependence of C−N bond length, d_{CN}, on N···O(N) interatomic distance, $d_{N\cdots O(N)}$, for variously substituted aniline/anilinium cation derivatives in their H-bonded complexes (experimental data retrieved from CSD).

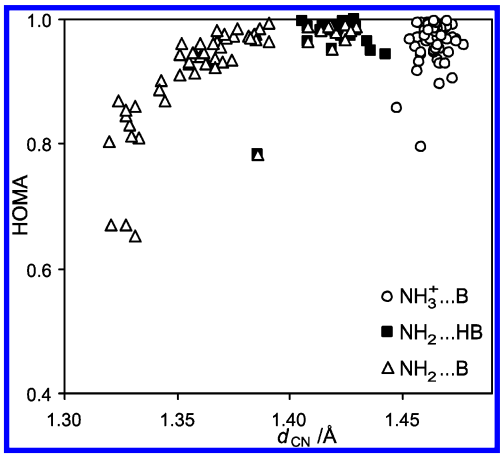

Figure 9. Dependence of HOMA on C−N bond length, d_{CN}, for variously substituted aniline/anilinium cation derivatives in their H-bonded complexes (experimental geometry retrieved from CSD).

of 0.005, 0.012, and 0.031, and mean values of the N···O(N) distance of 2.846, 2.783, and 2.996 Å (estimated standard deviations 0.091, 0.074, and 0.056) respectively for cases i, ii, and iii. In the solid phase, NH_2 and NH_3^+ groups may be involved in more than one hydrogen bond presented in Chart 1. It is nicely depicted in Figure 8, where for the same C−N bond length, ca. 1.420 Å, $NH_2\cdots HB$ and $NH_2\cdots B$ interactions coexist. In a large majority of these cases, the amino group acts as proton acceptor and donor simultaneously. A shorter N···O(N) interatomic distance for the $NH_2\cdots HB$ interaction than for the $NH_2\cdots B$ interaction is in agreement with calculation results for a 1:2 complex of methylamine with two molecules of water.[70]

The long-distance consequences of H-bonding on aromatic ring are illustrated by the relationship between d_{CN} and HOMA values. The shape of this dependence recalls that for phenol derivatives involved in H-bond complexation with bases.[14] It is important to note that qualitatively this is like the analogical scatter plot for optimized geometries (Figures 4 and S2). It is noteworthy to stress that the B3LYP results (Figure 4) are closer to X-ray data (Figure 9) than the MP2 results (Figure S2). The outlying points in Figure 9 (HOMA $\sim$ <0.8) refer to derivatives of aniline with ortho substituents acting as proton-accepting groups (NO_2 or COOH).[71]

All scatter plots presented in Figures 7−9 exhibit a substantial dispersion—they are strongly obscured by packing forces, which for weak interactions such as H-bonding may lead to remarkable distortions of its geometry.[15]

CONCLUSIONS

In conclusion, it should be pointed out that both experimental data from X-ray structure determination and computationally modeled results are in qualitative agreement. Additionally, a comparison of two levels of modeling shows that the B3LYP better reproduces experimental data than MP2, as it was shown earlier.[38,39] The most dramatic changes in the aromatic character of the ring are observed for H-bonded complexes where the N−H bond interacts with basic centers of other molecules [NH_2···B, Chart 1 (iii)] or the NH^- group interacts with HB [NH^-···HB; Chart 1 (iv)]. Two other kinds of complexes, with NH_2···HB and NH_3^+···B interactions, influence the aromaticity of the ring to a much smaller extent. Independently of the kind of H-bonding in which the NH^-, NH_2, or NH_3^+ groups are involved, the Bent−Walsh rule is approximately fulfilled.

ACKNOWLEDGMENT

The authors thank the Interdisciplinary Center for Mathematical and Computational Modeling (Warsaw, Poland) for computational facilities and the Warsaw University of Technology for financial support. KBN grant 3 T0 9A 03128 provided financial support for this study.

Supporting Information Available: (Table S1) Geometrical parameters (presented in Figure 1) for calculations B3LYP/6-311+G**. (Table S2 and Figure S1) Geometrical parameters and scatter plot of HOMA vs C−N bond length (Figure S2) for MP2/aug-cc-pVDZ calculation. The values of the H-bond interaction energy, BSSE correction, C−N bond length, and interatomic distance between the nitrogen and fluorine for B3LYP modeling interaction of aniline as NH^-···HF, NH_2···F^-, and NH_2···HF systems (Table S3). Statistical details of experimental (CSD) data (Table S4). Full geometric data and electronic energy (in au) for B3LYP optimized structures, that is, the Cartesian coordinates of 4-X-aniline, 4-X-anilinium cations and the 4-X-anilide anion, and their H-bonded complexes. Supplementary references including REFCODE of the data retrieved from CSD. This information is available free of charge via the Internet at http://pubs.acs.org

REFERENCES AND NOTES

(1) Minkin, V. I.; Glukhovtsev, M. N.; Simkin, B. Ya. *Aromaticity and Antiaromaticity*; John Wiley: New York, 1995.

(2) (a) Schleyer, P. v. R. Introduction: Aromaticity. *Chem. Rev.* **2001**, *101*, 1115−1117. (b) Buhl, M.; Hirsch, A. Spherical Aromaticity of Fullerenes. *Chem. Rev.* **2001**, *101*, 1153−1184. (c) Mitchell, R. H. Measuring Aromaticity by NMR. *Chem. Rev.* **2001**, *101*, 1301−1316. (d) Gomes, J. A. N. F.; Mallion, R. B. Aromaticity and Ring Currents. *Chem. Rev.* **2001**, *101*, 1349−1384. (e) Katritzky, A. R.; Jug, K.; Oniciu, D. C. Quantitative Measures of Aromaticity for Mono-, Bi-, and Tricyclic Penta- and Hexaatomic Heteroaromatic Ring Systems and Their Interrelationships. *Chem. Rev.* **2001**, *101*, 1421−1450. (f) de Proft, F.; Geerlings, P. Conceptual and Computational DFT in the Study of Aromaticity. *Chem. Rev.* **2001**, *101*, 1451−1464. (g) Jug, K.; Hiberty, P. C.; Shaik, S. $\sigma-\pi$ Energy Separation in Modern Electronic Theory for Ground States of Conjugated Systems. *Chem. Rev.* **2001**, *101*, 1477−1500. (h) Slayden, S. W.; Liebman, J. F. The Energetics of Aromatic Hydrocarbons: An Experimental Thermochemical Perspective. *Chem. Rev.* **2001**, *101*, 1541−1566.

(3) Krygowski, T. M.; Cyrański, M. K. Structural Aspects of Aromaticity. *Chem. Rev.* **2001**, *101*, 1385−1420.

(4) (a) Balaban, A. T.; Schleyer, P. V. R.; Rzepa, H. S. Crocker, Not Armit and Robinson, Begat the Six Aromatic Electrons. *Chem. Rev.* **2005**, *105*, 3436−3447. (b) Kertesz, M.; Choi, C. H.; Yang, S. Conjugated Polymers and Aromaticity. *Chem. Rev.* **2005**, *105*, 3448−3481. (c) Krygowski, T. M.; Stępien , B. T. Sigma- and Pi-Electron Delocalization: Focus on Substituent Effect. *Chem. Rev.* **2005**, *105*, 3482−3512. (d) Sobczyk, L.; Grabowski, S. J.; Krygowski, T. M. Interrelation between H-Bond and Pi-Electron Delocalization. *Chem. Rev.* **2005**, *105*, 1513−3560. (e) Raczyn ska, E. D.; Kosiñska, W.; Ośmiałowski, B.; Gawinecki, R. Tautomeric Equilibria in Relation to Pi-Electron Delocalization. *Chem. Rev.* **2005**, *105*, 3561−3612. (f) Cyrański, M. K. Energetic Aspects of Cyclic Pi-Electron Delocalization: Evaluation of the Methods of Estimating Aromatic Stabilization Energies. *Chem. Rev.* **2005**, *105*, 3773−3811. (g) Chen, Z.; Wannere, C. S.; Corminboeuf, C.; Puchta, R.; Schleyer, P. v. R. Nucleus-Independent Chemical Shifts (NICS) as an Aromaticity Criterion. *Chem. Rev.* **2005**, *105*, 3842−3888. (h) Poater, J.; Duran, M.; Sola, M.; Silvi, B. Theoretical Evaluation of Electron Delocalization in Aromatic Molecules by Means of Atoms in Molecules (AIM) and Electron Localization Function (ELF) Topological Approaches. *Chem. Rev.* **2005**, *105*, 3911−3947. (i) Bultinck, P.; Ponec, R.; Van Damme, S. Multicenter Bond Indices as a New Measure of Aromaticity in Polycyclic Aromatic Hydrocarbons. *J. Phys. Org. Chem.* **2005**, *18*, 706−718.

(5) (a) Lazzeretti, P. Assessment of Aromaticity via Molecular Response Properties. *Phys. Chem. Chem. Phys.* **2004**, *6*, 217−223. (b) Steiner, E.; Fowler, P. W. On the Orbital Analysis of Magnetic Properties. *Phys. Chem. Chem. Phys.* **2004**, *6*, 261−272. (c) Havenith, R. W. A.; Engelberts, J.; Fowler, P. W.; Steiner, E.; Van Lenthe, J. H.; Lazzeretti, P. Localization and Reversal of Paratropic Ring Currents in Molecules with Formal Anti-Aromatic Electrons Counts. *Phys. Chem. Chem. Phys.* **2004**, *6*, 289−294. (d) Poater, J.; Garcia-Cruz, I.; Illas, F.; Sola, M. Discrepancy between Common Local Measures in a Series of Carbazole Derivatives. *Phys. Chem. Chem. Phys.* **2004**, *6*, 314−318.

(6) Bultinck, P. Critical Analysis of the Local Aromaticity Concept in Polyaromatic Hydrocarbons. *Faraday Discuss.* **2007**, *135*, 347−365.

(7) (a) Lipkowitz, K. B.; Peterson, M. A. Benzene Is Not Very Rigid. *J. Comput. Chem.* **1993**, *14*, 121−125. (b) Dijkstra, F.; Van Lenthe, J. H. Aromaticity of Bent Benzene Rings: A VBSCF Study. *Int. J. Quantum Chem.* **1999**, *74*, 213−221. (c) Van Lenthe, J. H.; Havenith, R. W. A.; Dijkstra, F.; Jenneskens, L. W. 1,3,5-Cyclohexatriene Captured in Computro; the Importance of Resonance. *Chem. Phys. Lett.* **2002**, *361*, 203−208. (d) Poater, J.; Garcia-Cruz, I.; Illas, F.; Sola, M. Discrepancy between Common Local Aromaticity Measures in a Series of Carbazole Derivatives. *Phys. Chem. Chem. Phys.* **2004**, *6*, 314−318.

(8) (a) Domenicano, A.; Vaciago, A.; Coulson, C. A. Molecular Geometry of Substituted Benzene Derivatives. I. On the Nature of the Ring Deformation Induced by Substitution. *Acta Crystallogr., Sect. B: Struct. Sci.* **1975**, *31*, 221−234. (b) Domenicano, A.; Vaciago, A.; Coulson, C. A. Molecular Geometry of Substituted Benzene Derivatives. II. A Bond Angle versus Electronegativity Correlation for the Phenyl Derivatives of Second-Row Elements. *Acta Crystallogr., Sect. B: Struct. Sci.* **1975**, *31*, 1630−1641.

(9) Campanelli, A. R.; Domenicano, A.; Ramondo, F. Electronegativity, Resonance, and Steric Effects and the Structure of Monosubstituted Benzene Rings: An ab Initio Study. *J. Phys. Chem. A* **2003**, *107*, 6429−6440.

(10) Campanelli, A. R.; Domenicano, A.; Ramondo, F.; Hargittai, I. Group Electronegativities from Benzene Ring Deformation: A Quantum Chemical Study. *J. Phys. Chem. A* **2004**, *108*, 4940−4948.

(11) (a) Krygowski, T. M.; Ejsmont, K.; Stępień, B. T.; Cyrański, M. K.; Poater, J.; Solà, M. Relation between the Substituent Effect and Aromaticity. *J. Org. Chem.* **2004**, *69*, 6634−6640. (b) Suresh, C. H.; Koga, N. An Isodesmic Reaction Based Approach to Aromaticity of a Large Spectrum of Molecules. *Chem. Phys. Lett.* **2006**, *419*, 550−556.

(12) Krygowski, T. M.; Stępień, B. T. Changes in Aromaticity in the Ring of Monosubstituted Benzene Derivatives. *Pol. J. Chem.* **2004**, *78*, 2213−2217.

(13) Krygowski, T. M.; Stępień, B. T.; Cyrański, M. K; Ejsmont, K. Relation between Resonance Energy and Substituent Resonance Effect in P-Phenols. *J. Phys. Org. Chem.* **2005**, *18*, 886−891.

(14) Krygowski, T. M.; Zachara, J. E.; Szatyłowicz, H. Molecular Geometry as a Source of Chemical Information. Part III. How H-Bonding Affects Aromaticity of the Ring in the Case of Phenol and Para-Nitrophenol Complexes − a B3LYP/6−311+G** Study. *J. Org. Chem.* **2004**, *69*, 7038−7043.

(15) Krygowski, T. M.; Szatyłowicz, H.; Zachara, J. E. How H-Bonding Affects Aromaticity of the Ring in Variously Substituted Phenol Complexes with Bases. 4. Molecular Geometry as a Source of Chemical Information. *J. Chem. Inf. Comput. Sci.* **2004**, *44*, 2077−2082.

(16) Krygowski, T. M.; Szatyłowicz, H.; Zachara, J. E. Molecular Geometry as a Source of Chemical Information. 5. Substituent Effect on Proton Transfer in Para-Substituted Phenol Complexes with Fluoride − a B3LYP/6−311+G** Study. *J. Chem. Inf. Model.* **2005**, *45*, 652−656.

(17) Krygowski, T. M. Crystallographic Studies of Inter- and Intramolecular Interactions Reflected in Aromatic Character of Pi-Electron Systems. *J. Chem. Inf. Comput. Sci.* **1993**, *33*, 70−78.

(18) Schleyer, P. v. R.; Maerker, C.; Dransfeld, A.; Jiao, H.; Hommes, N. J. R. V. E. Nucleus-Independent Chemical Shifts: A Simple and Efficient Aromaticity Probe. *J. Am. Chem. Soc.* **1996**, *118*, 6317−6318.

(19) Schleyer, P. v. R.; Manoharan, M.; Wang, Z. -X.; Kiran, B.; Jiao H.; Puchta, R.; Hommes, N. J. R. v. E. Dissected Nucleus-Independent Chemical Shift Analysis of π-Aromaticity and Antiaromaticity. *Org. Lett.* **2001**, *3*, 2465−2468.

(20) Corminboeuf, C.; Heine, T.; Seifert, G.; Schleyer, P. v. R.; Weber. J. Induced Magnetic Fields in Aromatic [n]-Annulenes − Interpretation of NICS Tensor Components. *Phys. Chem. Chem. Phys.* **2004**, *6*, 273−276.

(21) Perrin, D. D. *Dissociation Constants of Organic Bases in Aqueous Solution: Supplement 1972*. Butterworths: London, 1972.

(22) Bordwell, F. G. Equilibrium Acidities in Dimethyl Sulfoxide Solution. *Acc. Chem. Res*. **1988**, *21*, 456−463.

(23) Kamlet, M. J.; Taft, R. W. The Solvatochromic Comparison Method. I. The β-Scale of Solvent Hydrogen-Bond Acceptor (HBA) Basicities. *J. Am. Chem. Soc*. **1976**, *98*, 377−383.

(24) Reichardt, C. *Solvents and Solvent Effects in Organic Chemistry*; Wiley-VCH: Weinheim, Germany, 2003, (a) pp 421, 423; (b) pp 99−106.

(25) Krygowski, T. M.; Fawcett, R. W. Complementary Lewis Acid-Base Description of Solvent Effect. I. Ion−Ion and Ion−Dipole Interactions. *J. Am. Chem. Soc*. **1975**, *97*, 2143−2148.

(26) Szatyłowicz, H.; Krygowski, T. M.; Hobza, P. How the Shape of the NH_2 Group Depends on the Substituent Effect and H-Bond Formation in Derivatives of Aniline. *J. Phys. Chem. A* **2007**, *111*, 170−175.

(27) (a) Jeffrey, G. A. *An Introduction to Hydrogen Bonding*; Oxford University Press: Oxford, New York, 1997. (b) Scheiner, S. *Hydrogen Bonding, A Theoretical Perspective*; Oxford University Press: Oxford, New York, 1997. (c) Perrin, C. L. Symmetries of Hydrogen Bond in Solution. *Science* **1994**, *266*, 1665−1668. (d) Steiner, T. The Hydrogen Bond in the Solid State. *Angew. Chem., Int. Ed.* **2002**, *41*, 48−76. (e) Grabowski, S. J. Hydrogen Bonding Strength − Measures Based on Geometric and Topological Parameters. *J. Phys. Org. Chem*. **2004**, *17*, 18−31.

(28) (a) Jeffrey, G. A.; Saenger, W. *Hydrogen Bonding in Biological Structures*; Springer: Berlin, 1991. (b) Desiraju, G. R.; Steiner, T. *The Weak Hydrogen Bonding in Structural Chemistry and Biology*; Oxford University Press: Oxford, New York, 1999. (c) Meyer, E. A.; Castellano, R. K.; Diederich, F. Interactions with Aromatic Rings in Chemical and Biological Recognition. *Angew. Chem., Int. Ed*. **2003**, *42*, 1210−1250.

(29) Szatyłowicz, H.; Krygowski, T. M. Molecular Geometry as a Source of Chemical Information. Part I: How H-Bonding Modifies Molecular Structure in the Vicinity of Hydrogen Donating Group. The Case of Phenol Derivatives Interacting with Nitrogen and Oxygen Bases. *Pol. J. Chem*. **2004**, *78*, 1719−1731.

(30) Krygowski, T. M.; Szatyłowicz, H.; Zachara, J. E. How H-Bonding Modifies Molecular Structure and π-Electron Delocalization in the Ring of Pyridine/Pyridinium Derivatives Involved in H-Bond Complexation. *J. Org. Chem.* **2005**, *70*, 8859−8865.

(31) Allen, F. H. The Cambridge Structural Database: A Quarter of a Million Crystal Structures and Rising. *Acta Crystallogr., Sect. B: Struct. Sci*. **2002**, *58* (3 PART 1), 380−388.

(32) Krygowski, T. M.; Zachara, J. E.; Szatyłowicz, H. Molecular Geometry as a Source of Chemical Information. Part 2: An Attempt to Estimate the H-Bond Strength - the Case of p-Nitrophenol Complexes with Bases. *J. Phys. Org. Chem.* **2005**, *18*, 110−114.

(33) Bondi, A. Van der Waals Volumes and Radii. *J. Phys. Chem.* **1964**, *68*, 441−451.

(34) (a) Lee, C.; Yang, W.; Parr, R. G. Development of the Colle-Salvetti Correlation-Energy Formula into a Functional of the Electron Density. *Phys. Rev. B: Condens. Matter Mater. Phys.* **1988**, *37*, 785−789. (b) Becke, A. D. A New Mixing of Hartree−Fock and Local Density-Functional Theories. *J. Chem. Phys.* **1993**, *98*, 1372−1377. (c) Becke, A. D. Density-Functional Thermochemistry. III. The Role of Exact Exchange. *J. Chem. Phys.* **1993**, *98*, 5648−5652. (d) Stephens, P. J.; Devlin, F. J.; Chabalowski, C. F.; Frisch, M. J. Ab Initio Calculation of Vibrational Absorption and Circular Dichroism Spectra Using Density Functional Force Fields. *J. Phys. Chem.* **1994**, *98*, 11623−11627.

(35) (a) McLean, A. D.; Chandler, G. S. Contracted Gaussian Basis Sets for Molecular Calculations. I. Second Row Atoms, Z=11−18. *J. Chem. Phys.* **1980**, *72*, 5639−5648. (b) Krishnan, R.; Binkley, J. S.; Seeger, R.; Pople, J. A. Self-Consistent Molecular Orbital Methods. XX. A Basis Set for Correlated Wave Functions. *J. Chem. Phys.* **1980**, *72*, 650−654. (c) Clark, T.; Chandrasekhar, J.; Spitznagel, G. W.; Schleyer, P. v. R. Efficient Diffuse Function-Augmented Basis Sets for Anion Calculations. III. The 3-21+G Basis Set for First-Row Elements, Li−F. *J. Comput. Chem.* **1983**, *4*, 294−301. (d) Frisch, M. J.; Pople, J. A.; Binkley, J. S. Self-Consistent Molecular Orbital Methods. 25. Supplementary Functions for Gaussian Basis Sets. *J. Chem. Phys.* **1984**, *80*, 3265−3269.

(36) (a) Moller, C.; Plesset, M. S. Note on an Approximation Treatment for Many-Electron Systems. *Phys. Rev.* **1934**, *46*, 618−622. (b) Krishnan, R.; Pople, J. A. Approximate Fourth-Order Perturbation Theory of the Electron Correlation Energy. *Int. J. Quantum Chem*. **1978**, *14*, 91−100.

(37) (a) Dunning, T. H., Jr. Gaussian Basis Sets for Use in Correlated Molecular Calculations. I. The Atoms Boron through Neon and Hydrogen. *J. Chem. Phys*. **1989**, *90*, 1007−1023. (b) Kendall, R. A.; Dunning, T. H., Jr.; Harrison, R. J. Electron Affinities of the First-Row Atoms Revisited. Systematic Basis Sets and Wave Functions. *J. Chem. Phys*. **1992**, *96*, 6796−6806. (c) Woon, D. E.; Dunning, T. H., Jr. Gaussian Basis Sets for Use in Correlated Molecular Calculations. III. The Atoms Aluminum Through Argon. *J. Chem. Phys*. **1993**, *98*, 1358−1371.

(38) Vaschetto, M. E.; Retamal, B. A.; Monkman, A. P. Density Functional Studies of Aniline and Substituted Anilines. *THEOCHEM* **1999**, *468*, 209−221.

(39) (a) Wojciechowski, P. M.; Zierkiewicz, W.; Michalska, D.; Hobza, P. Electronic Structures, Vibrational Spectra, and Revised Assignment of Aniline and its Radical Cation: Theoretical Study. *J. Chem. Phys*. **2003**, *118*, 10900−10911. (b) Palafox, M. A.; Gill, M.; Nunez, N. J.; Rastogi, V. K.; Mittal, L.; Sharma, R. Scaling Factors for the Prediction of Vibrational Spectra. II. The Aniline Molecule and Several Derivatives. *Int. J. Quantum Chem*. **2005**, *103*, 394−421.

(40) Fallah-Bagher-Shaidaei, H.; Wannere, C. S.; Corminboeuf, C.; Puchta, R.; Schleyer, P. v. R. Which NICS Aromaticity Index for Planar π Rings Is Best? *Org. Lett.* **2006**, *8*, 863−866.

(41) Frisch, M. J.; Trucks, G. W.; Schlegel, H. B.; Scuseria, G. E.; Robb, M. A.; Cheeseman, J. R.; Montgomery, J. A., Jr.; Vreven, T.; Kudin, K. N.; Burant, J. C.; Millam, J. M.; Iyengar, S. S.; Tomasi, J.; Barone, V.; Mennucci, B.; Cossi, M.; Scalmani, G.; Rega, N.; Petersson, G. A.; Nakatsuji, H.; Hada, M.; Ehara, M.; Toyota, K.; Fukuda, R.; Hasegawa, J.; Ishida, M.; Nakajima, T.; Honda, Y.; Kitao, O.; Nakai, H.; Klene, M.; Li, X.; Knox, J. E.; Hratchian, H. P.; Cross, J. B.; Adamo, C.; Jaramillo, J.; Gomperts, R.; Stratmann, R. E.; Yazyev, O.; Austin, A. J.; Cammi, R.; Pomelli, C.; Ochterski, J. W.; Ayala, P. Y.; Morokuma, K.; Voth, G. A.; Salvador, P.; Dannenberg, J. J.; Zakrzewski, V. G.; Dapprich, S.; Daniels, A. D.; Strain, M. C.; Farkas, O.; Malick, D. K.; Rabuck, A. D.; Raghavachari, K.; Foresman, J. B.; Ortiz, J. V.; Cui, Q.; Baboul, A. G.; Clifford, S.; Cioslowski, J.; Stefanov, B. B.; Liu, G.; Liashenko, A.; Piskorz, P.; Komaromi, I.; Martin, R. L.; Fox, D. J.; Keith, T.; Al-Laham, M. A.; Peng, C. Y.; Nanayakkara, A.; Challacombe, M.; Gill, P. M. W.; Johnson, B.; Chen, W.; Wong, M. W.; Gonzalez, C.; Pople, J. A. *Gaussian 03*, Revision C.02; Gaussian, Inc.: Wallingford, CT, 2004.

(42) Kruszewski, J.; Krygowski, T. M. Definition of Aromaticity Basing on the Harmonic Oscillator Model. *Tetrahedron Lett.* **1972**, 3839−3842.

(43) Julg, A.; François, P. Recherches sur la Géométrie de Quelques Hydrocarbures Non-Alternants: Son Influence sur les Énergies de Transition, une Nouvelle Définition de l'Aromaticité (Geometry of Nonalternant Hydrocarbons: Its Influence on the Transition Energies, a New Definition of Aromaticity). *Theor. Chim. Acta* **1967**, *8*, 249−259.

(44) Foresman, J. B.; Frish, E. Studying Chemical Reaction and Reactivity. In *Exploring Chemistry with Electronic Structure Methods*, 2nd ed.; Gaussian Inc.: Pittsburgh, 1996; pp 165−211.

(45) (a) Tawa, G. J.; Topol, I. A.; Burt, S. K.; Caldwell, R. A.; Rashin, A. A. Calculation of the Aqueous Solvation Free Energy of the Proton. *J. Chem. Phys*. **1998**, *109*, 4852−4863. (b) Topol, I. A.; Tawa, G. J.; Caldwell, R. A.; Eissenstat, M. A.; Burt, S. K. Acidity of Organic Molecules in the Gas Phase and in Aqueous Solvent. *J. Phys. Chem. A* **2000**, *104*, 9619−9624. (c) Pokon, E. K.; Liptak, M. D.; Feldgus, S.; Shields, G. C. Comparison of CBS-QB3, CBS-APNO, and G3 Prediction of Gas Phase Deprotonation Data. *J. Phys. Chem. A* **2001**, *105*, 10483−10487. (d) Liptak, M. D.; Shields, G. C. Accurate pKa Calculation for Carboxylic Acids Using Complete Basis Set and Gaussian-n Models Combined with CPCM Continuum Solvation Methods. *J. Am. Chem. Soc.* **2001**, *123*, 7314−7319.

(46) Boys, S. F.; Bernardi, F. The Calculation of Small Molecular Interactions by the Differences of Separate Total Energies. Some Procedures with Reduced Errors. *Mol. Phys*. **1970**, *19*, 553−566.

(47) (a) Arnet, E. M. Gas-Phase Proton Transfer. Breakthrough for Solution Chemistry. *Acc. Chem. Res*. **1973**, *6*, 404−409. (b) Taft, R. W. Gas Phase Proton Transfer. In *Proton Transfer Reactions*; Caldin, E. F., Gold, V., Eds.; Chapman and Hall: London 1975, pp 31−77.

(48) Larson, J. W.; McMahon, T. B. Strong Hydrogen Bonding in Gas-Phase Anions. An Ion Cyclotron Resonance Determination of Fluoride Binding Energetics to Broensted Acids from Gas-Phase Fluoride Exchange Equilibria Measurements. *J. Am. Chem. Soc*. **1983**, *105*, 2944−2950.

(49) Taft, R. W.; Topsom, R. D. The Nature and Analysis of Substituent Electronic Effects. *Prog. Phys. Org. Chem*. **1987**, *16*, 1−83.

(50) Alkorta, I.; Rozas, I.; Mo, O.; Yanez, M.; Elguero, J. Hydrogen Bond vs Proton Transfer between Neutral Molecules in the Gas Phase. *J. Phys. Chem. A* **2001**, *105*, 7481−7485.

(51) Bernstein, J. Effect of Crystal Environmental on Molecular Structure. In *Accurate Molecular Structures*; Domenicano, A., Hargittai, I., Eds.; Oxford University Press: New York, 1992; pp 469−497.

(52) *NIST Chemistry WebBook, NIST Standard Reference Database Number 69*; Linstrom, P. J., Mallard, W. G., Eds.; National Institute of Standards and Technology: Gaithersburg MD, June 2005; 20899. http://webbook.nist.gov/chemistry (accessed Mar 2007).

(53) Bartmess, J. E.; Scott, J. A.; McIver, R. T., Jr. Scale of Acidities in the Gas Phase from Methanol to Phenol. *J. Am. Chem. Soc*. **1979**, *101*, 6046−6056.

(54) Blondel, C.; Delsart, C.; Goldfarb, F. Electron Spectrometry at the meV Level and the Electron Affinities of Si and F. *J. Phys. B: At., Mol. Opt. Phys.* **2001**, *34*, L281−L288.

(55) Bradforth, S. E.; Kim, E. H.; Arnold, D. W.; Neumark, D. M. Photoelectron Spectroscopy of CN^-, NCO^-, and NCS^-. *J. Chem. Phys.* **1993**, *98*, 800−810.

(56) Hunter, E. P.; Lias, S. G. Evaluated Gas Phase Basicities and Proton Affinities of Molecules: An Update. *J. Phys. Chem. Ref. Data* **1998**, *27*, 413−656.

(57) Hillebrand, C.; Klessinger, M.; Ecker-Maksic, M.; Maksic, Z. B. Theoretical Model Calculations of the Proton Affinities of Aminoalkanes, Aniline, and Pyridine. *J. Phys. Chem*. **1996**, *100*, 9698−9702.

(58) Swart, M.; Bickelhoupt, M. Proton Affinities of Anionic Bases: Trends Across the Periodic Table, Structural Effects, and DFT Validation. *J. Chem. Theory Comput.* **2006**, *2*, 281−287.

(59) Ervin, K. M.; DeTuri, V. P. Anchoring the Gas-Phase Acidity Scale. *J. Phys. Chem. A* **2002**, *106*, 9947−9956.

(60) (a) Merrill, G. N.; Kass, S. R. Calculated Gas-Phase Acidities Using Density Functional Theory: Is It Reliable? *J. Phys. Chem*. **1996**, *100*, 17465−17471. (b) Burk, P.; Koppel, I. A.; Koppel, I.; Leito, I.; Travnikova, O. Critical Test of Performance of B3LYP Functional for Prediction of Gas-Phase Acidities and Basicities. *Chem. Phys. Lett*. **2000**, *323*, 482−489. (c) Fu, Y.; Liu, L.; Li, R.-Q.; Liu, R.; Gou, Q. -X. First-Principle Predictions of Absolute pKa's of Organic Acids in Dimethyl Sulfoxide Solution. *J. Am. Chem. Soc*. **2004**, *126*, 814−822.

(61) Note that dissociation of water leads to concentration of H_3O^+ and OH^- at a level of 10^{-7} mol/dcm^{-3}, and despite this, both of these chemical entities are the subject of numerous studies, including structural ones. Moreover, small concentrations of chemical species may be of great importance for kinetically controlled chemical reactions!

(62) Krygowski, T. M.; Szatyłowicz, H. Varying Electronegativity of OH/O^- Groups Depending on the Nature and Strength of H-Bonding in Phenol/Phenolate Involved in H-Bond Complexation. *J. Phys. Chem. A* **2006**, *110*, 7232−7236.

(63) (a) Walsh, A. D. The Properties of Bonds Involving Carbon. *Discuss. Faraday Soc*. **1947**, *2*, 18−25. (b) Bent, H. A. An Appraisal of Valence-Bond Structures and Hybridization in Compounds of the First-Row Elements. *Chem. Rev*. **1961**, *61*, 275−311.

(64) Wilson, E. B.; Decius, J. C.; Cross, P. C. *Molecular Vibrations − The Theory of Infrared and Raman Vibrational Spectra*; McGraw−Hill: New York, 1955; p 175.

(65) Mulliken, R. S. Electronic Population Analysis on LCAO-MO Molecular Wave Functions. I. *J. Chem. Phys*. **1955**, *23*, 1833−1840.

(66) Cyrañski, M. K.; Krygowski, T. M.; Katritzky, A. R.; Schleyer, P. v. R. To What Extent Can Aromaticity Be Defined Uniquely? *J. Org. Chem*. **2002**, *67*, 1333−1338.

(67) Cochran; W. G.; Snedecor, G. W. *Statistical Methods*; The Iowa State University Press: Ames, IA, 1973.

(68) (a) Baker, J. W. *Hyperconjugation*; Oxford University Press: Oxford, U. K., 1952. (b) Pophristic, V.; Goodman, L. Hyperconjugation not Steric Repulsion Leads to the Staggered Structure of Ethane. *Nature* **2001**, *411*, 565−568.

(69) (a) Speakman, J. C. Acid Salts of Carboxylic Acids, Crystals with Some "Very Short" Hydrogen Bonds. *Struct. Bonding* **1972**, *12*, 141−199. (b) Emsley, J. Very Strong Hydrogen Bonding. *Chem. Soc. Rev*. **1980**, *9*, 91−124. (c) Bertolasi, V.; Gilli, P.; Ferretti, V.; Gilli, G. Evidence for Resonance-Assisted Hydrogen Bonding. 2. Intercorrelation between Crystal Structure and Spectroscopic Parameters in Eight Intramolecularly Hydrogen Bonded 1,3-Diaryl-1,3-Propanedione Enols. *J. Am. Chem. Soc*. **1991**, *113*, 4917−4925.

(70) Mmereki, B. T.; Donaldson, D. J. Ab Initio and Density Functional Study of Complexes between the Methylamines and Water. *J. Phys. Chem. A* **2002**, *106*, 3185−3190.

(71) (a) Ammon, H. L.; Bhattacharjee, S. K. Crystallographic Studies of High-Density Organic Compounds: 3,5-Diamino-2,4,6-trinitrobenzamide. *Acta Crystallogr., Sect. B: Struct. Sci*. **1982**, *38*, 2083−2086. (b) Brown, C. J.; Ehrenberg, M. Anthranilic Acid, $C_7H_7NO_2$, by Neutron Diffraction. *Acta Crystallogr., Sect. C: Cryst. Struct. Commun*. **1985**, *41*, 441−443. (c) Ammon, H. L.; Prasad, S. M. 3,5-Diamino-2,4,6-trinitrobenzoic Acid, $C_7H_5N_5O_8$. *Acta Crystallogr., Sect. C: Cryst. Struct. Commun*. **1985**, *41*, 921−924.

CI600502W